Supplemental Materials

MATERIALS AND METHODS

Peptides synthesis and stock preparation

R321 and R323 were synthesized on a Liberty Blue Microwave peptide synthesizer (CEM Corporation) using Fmoc chemistry and low loading Rink Amide MBHA resin (Merck). The following modifications have been introduced to the published protocol of high efficiency peptide synthesis (http://www.ncbi.nlm.nih.gov/pubmed/24456219): The coupling with N,N'-Diisopropylcarbodiimide (DIC)/ ethyl 2-cyano-2-(hydroxyimino) acetate (OXYMA) was performed for 4 min at 90^{o}C for all residue except for His, for which the reaction was carried out for 10 min at 50^{o}C. A 5-fold amino acid excess was used on all cycles and all residues were double-coupled. All deprotection cycles were conducted at room temperature to avoid racemization and aspartimide formation. Due to the high cost of Fmoc-NH-$(PEG)_{27}$-COOH (Merck), it was attached manually overnight using 1.2-fold excess and HCTU as an activating agent. The peptides were cleaved from the resin and deprotected with a mixture of 90.0% (v/v) trifluoroacetic acid (TFA) with 2.5% water, 2.5% triisopropyl-silane, 2.5% 2,2′-(ethylenedioxy)diethanethiol and 5% thioanisol. Peptides were purified on a preparative (25 mm × 250 mm) Atlantis C3 reverse phase column (Agilent Technologies) in a 90 min gradient of 0.1% (v/v) trifluoroacetic acid in water and 0.1% trifluoroacetic acid in acetonitrile, with a 10 mL/min flow rate. The fractions containing peptides were analyzed on Agilent 6100 LC/MS spectrometer with the use of a Zorbax 300SB-C3 PoroShell column and a gradient of 5% acetic acid in water and acetonitrile. Fractions that were more than 95% pure were

combined and freeze dried. Peptides stock solution was prepared by dissolving in DMSO or DMSO-d_6 (for NMR experiments). Upon reconstitution in PBS, pH 7.2, the final concentration of DMSO was less than 1%. The solutions were sonicated, kept at room temperature overnight, centrifuged and stored at -20ºC.

Dynamic Light Scattering (DLS)

Peptides were resuspended in 100% DMSO to a concentration of 1 mM and then further diluted in PBS to a final concentration of 10 µM. The hydrodynamic radius of the peptides was measured on a DynaPro-801 (Protein Solutions, Charlottesville, VA) molecular size detector and the data was analyzed with the provided software using an aqueous buffer model.

Chemotaxis Assays

Optimal concentrations of chemokines (12 nM CCL11, 25 nM CCL24, 100 nM CCL26, and 1 µM platelet-activating factor, PAF) were used to induce cell chemotaxis .[1, 2] CCL11, CCL24, and CCL26 were purchased from BioLegend (San Diego, CA) and PAF (C16) was purchased from Tocris Bioscience (Minneapolis, MN). Inhibitors or controls were placed in both upper and lower chambers of transwell plates with 5 µm pore size membranes (Corning, Kennebunk, ME). For assays used to determine the effect of R321 on the chemotaxis of human peripheral blood eosinophils toward PAF, a PAF receptor inhibitor WEB 2086 was purchased from Tocris Bioscience (Minneapolis, MN) and used at a concentration of 100 µM as a positive control. A total of $1x10^5$ cells were

placed in each well and following 4h of migration cells were counted using flow cytometry (Beckman Quanta SC, Beckman Coulter, Indianapolis, IN).

CCL11-induced secretion of ECP

Purified human peripheral blood eosinophils were resuspended in PBS + 0.1% BSA to a final concentration of 1x 10^6 cells/mL and 100 µL were aliquoted per well. Cells were pretreated for 30 min with 1 µM R321, R323, or vehicle, and stimulated with 12 nM CCL11 for 3h. Following stimulation, cells were centrifuged (1500 rpm, 10 min) and supernatants were collected for further analysis. ECP detection in supernatants was performed using a commercial ELISA kit (MesaCup ECP test, MBL, Woburn, MA).

Detection of ERK 1/2 and AKT

AML14.3D10-CCR3 cells were serum starved for 4h, resuspended in RPMI 1640 + 0.1% BSA to a density of 1x10^7 cells/mL, and then pretreated with either vehicle control (PBS + 1% DMSO) or 10 µM inhibitors (R321, R323, SB238437, or UCB35625) for 30 min at 37℃ and 5% CO_2. Cell aliquots were taken before stimulation and 2.5, 5, 10, 15, and 30 min after stimulation with 100 nM CCL11 and washed in ice cold PBS. Cell pellets were lysed in RIPA lysis buffer (Santa Cruz Biotechnology, Santa Cruz, CA) containing 1mM PMSF, 1mM Na-orthovanadate, 30 mM NaF, and protease inhibitor cocktail tablet (Roche, Indianapolis, IN). Cell lysate proteins were separated on 12% (w/v) SDS-PAGE gels (15µg/ lane) and transferred to PVDF membranes at 20V for 40 min. Membranes were blocked with 5% BSA for 2h at RT, and incubated overnight at +4℃ with rabbit anti-phospho-ERK 1/2 antibodies or rabbit anti-phospho-AKT

antibodies (Cell Signaling Technology, Danvers, MA). The next day, membranes were extensively washed and incubated for 1h at RT with secondary goat anti-rabbit IgG-HRP antibodies (Santa Cruz Biotechnology, Dallas, TX). Western blots were visualized using SuperSignal West Dura Extended Duration Substrate (Thermo Fisher Scientific, Waltham, MA). For loading controls, membranes were stripped for 15 min in mild stripping buffer (1.5% glycine, 0.1% SDS, 1% Tween-20, pH 2.2) and reprobed with rabbit anti-ERK 1/2 antibodies or rabbit anti-AKT antibodies (Cell Signaling Technology, Danvers, MA). Three independent experiments were performed.

Gαi activation

GTP-bound Gαi was detected using a commercial Gαi assay kit (Abcam, Cambridge, MA) with modifications. Briefly, AML14.3D10-CCR3 cells were serum-starved for 16h before being pretreated with 200 ng/ml pertussis toxin for 2h, 10 μM R321 for 30 min, or with vehicle control. Pretreated cells were then stimulated with 8 nM CCL11 or medium for 1 min. The reaction was stopped by adding and washing once in ice cold PBS. Ten (10) million cells were used for each condition. Washed cells were lysed with 1x lysis buffer following manufacturer instructions. For pull-down of active Gαi, mouse anti-GTP bound Gαi antibody was conjugated to Dynabeads Protein G (Life Technologies, Carlsbad, CA) for 15 min at RT. Conjugated beads were washed 3 times with TBST and incubated with cell lysates for 20min at RT. After washing with TBST, bound proteins were eluted by boiling the beads in 2x SDS sample buffer for 5 min. Eluates were resolved by SDS-PAGE and immunoblotted using a polyclonal rabbit anti-total Gαi antibody (Cell Signaling Technology, Danvers, MA).

CCR3 degradation

AML14.3D10-CCR3 cells were resuspended in RPMI1640 + 0.1% BSA. Aliquots of $1x10^6$ cells were pretreated with 10 µM cycloheximide for 1h at 37℃. Some cells were concurrently pretreated with 10 µM R321 for 30 min. Pretreated cells were stimulated with 8 nM CCL11/eotaxin-1 or CCL5/RANTES for 3h to induce receptor degradation. Cells were lysed in RIPA buffer and immunoblotted for CCR3 using a polyclonal rabbit anti-CCR3 antibody (Abcam, Cambridge, MA) followed by goat anti-rabbit IgG-HRP secondary antibody (Santa Cruz Biotechnology, Santa Cruz, CA).

Immunofluorescence and Confocal Microscopy

AML14.3D10-CCR3 cells were serum starved for 4h and then resuspended in RPMI 1640 + 0.1% BSA to a density of $1x10^6$ cells/mL. Cells were pretreated with 10 µM inhibitors (R321, SB238437 or UCB35625) or R323 or vehicle controls for 30 min at 37℃ and then stimulated with 100 nM CCL11. Aliquot s were taken before stimulation and 30 min after chemokine addition. Cytospin preparations were made by centrifugation of the treated cells at 300 rpm (10.16x g) for 5 min onto glass slides in a cytocentrifuge (Cytospin 2, Shandon, Pittsburgh, PA). Cells were fixed in ice cold methanol for 15 min at -20℃ and washed 3 times in 0.1% Triton X-100 in PBS before blocking in 10% normal goat serum in PBS for 2h at RT. The slides were incubated overnight at +4℃ with primary antibodies diluted i n 0.1% normal goat serum in PBS. CCR3 was detected with 5 µg/mL mouse anti-human CCR3 antibody (Biolegend, San Diego, CA) and β-arrestin 2 with rabbit monoclonal anti-human β-arrestin 2 antibody (Cell Signalling Technology, Danvers, MA). After extensive washing in 0.1% Tween-

20, samples were incubated with appropriate AlexaFluor®488- or AlexaFluor®568-conjugated anti-mouse and anti-rabbit secondary antibodies (Cell Signaling Technology, Danvers, MA) used at 1:500 dilution for 1h at RT. After washing, coverslips were mounted on the glass slides with SlowFade Gold antifade reagent with DAPI (Invitrogen, Carlsbad, CA). Images were collected with a Zeiss LSM 700 laser scanning confocal microscope and 100x/1.45 oil immersion objective using Zen software (Carl Zeiss AG, Oberkochen, Germany) and further processed with Photoshop CS5 (Adobe, San Jose, CA). Quantitative colocalization analysis was performed by selecting single cells as regions of interest (n=50 per treatment group) and calculating mean colocalization coefficients by Pearson's correlation method. Data is presented as mean ± SEM. Statistical analysis was performed using GraphPad Prism software (GraphPad, San Diego, CA) by two-way analysis of variance (ANOVA), followed by Tukey *post hoc* analysis.

Cell surface staining and gating strategy for mouse blood eosinophils

Mouse blood (900 µL) was collected by cardiac puncture into EDTA-coated tubes and red blood cell lysis was performed via hypotonic shock with H_2O. White blood cells were washed with PBS and resuspended to 1x 10^6 cells/100 µL of flow cytometry buffer (PBS + 0.1% BSA). Inhibition of non-specific binding to Fc receptors was performed using a rat anti-mouse CD16/CD32 antibody for 5 min at room temperature (BD Biosciences, San Jose, CA). Cells were subsequently stained for 30 min at RT in the dark with the following antibodies: rat anti-mouse CCR3 fluorescein-conjugated antibody (R&D Systems, Minneapolis, MN), PE-conjugated rat anti-mouse Siglec-F antibody (BD

Biosciences, San Jose, CA), and rat anti-mouse PerCP-Cyanine 5.5 Ly-6G (Gr1) antibody (Thermo Fisher Scientific, Waltham, MA). Cells were washed 3x in PBS, resuspended in 2% paraformaldehyde and analyzed immediately on a Quanta SC flow cytometer (Beckman Coulter, Indianapolis, IN). Eosinophils were gated from live cells as SSC^{hi}, Siglec F–CCR3 double positive, $Gr1^{Lo\text{-}neg}$. Results were analyzed using FlowJo software (FlowJo LLC, Ashland, OR).

Bronchoalveolar lavage (BAL)

One day after the last DRA allergen or sham PBS challenge, mice were euthanized and BAL cells were collected by lavage with 2 mL of cold PBS injected into the trachea via a catheter. Total cell counts were performed using a Countess automated cell counter (Thermo Fisher Scientific, Waltham, MA). For differential BAL cell counts, cytospin preparations were stained with Wright-Giemsa stain (Sigma- Aldrich, St. Louis, MO). Cells were classified as macrophages, lymphocytes, neutrophils, and eosinophils by standard morphology and staining. A minimum of 200 cells were counted per slide.

Determination of airway responsiveness to methacholine

Twenty-four hours after the last intranasal challenge, mice were anesthetized and attached to the FlexiVent rodent ventilator/pulmonary mechanics analyzer (Scireq, Montreal, Canada). Baseline respiratory parameters were measured as previously described.[3] Airway reactivity was assessed by measuring response to increasing doses (0, 5, 10, 20, and 40 µg) of methacholine (Sigma, St Louis, MO) administered intravenously via the jugular vein.

Reductive Methylation of Membrane Preparations.

ChemiSCREEN Chem-1 membrane preparations for recombinant human CCR3 (HTS008M) and negative control (HTS000MC1) CCR3-null membranes were purchased from EMD Millipore. Membrane preparation storage buffer contained 50 mM Tris pH 7.4, 10% glycerol and 1% BSA. Glycerol and BSA are important components for the stability and integrity of the membranes, however BSA and Tris interfere with the reductive methylation reaction. Therefore, ^{13}C formaldehyde (catalog # 489417, Aldrich) and borane–ammonia complex (Catalog #682098, Aldrich) were used in excess to ensure labeling of all possible components of the membranes. Upon quenching the reaction with excess Tris-HCl buffer, membrane fractions were separated by ultracentrifugation at 4℃ and the membrane pellets were resuspended in PBS containing 10% glycerol and 1% unlabeled BSA [4]. The latter step was repeated to remove residual labeled components. Reductive methylation of the membrane preparations was performed as described previously [5, 6]. In brief, 20 µl of 1 M borane–ammonia complex (Catalog #682098, Aldrich) and 40 µl of 1 M ^{13}C formaldehyde (Catalog #489417, Aldrich) were added to 1 ml of membrane preparation. This mixture was incubated with stirring for 2 h at 4℃. The addition of borane–ammonia and formaldehyde was repeated, and the mixture was incubated with stirring for 2 more hours. The final 10 µl 1 M borane – ammonia complex was then added and the mixture was incubated at 4℃ overnight with stirring. The reaction was then stopped by adding 110 µl of 2 M Tris·HCl (pH 7.6). Thereafter, the membrane preparations were separated by ultracentrifugation at 4℃ and resuspended in PBS containing 10% glycerol and 1% unlabeled BSA to be used for NMR experiments.

Heteronuclear Single Quantum Coherence (HSQC) NMR

Final samples (200 µl) contained 50% membrane preparation, 10% D_2O (Catalog #151882, Aldrich), 2% DMSO-d_6 (Catalog #156914, Aldrich). CCL11 (eotaxin) was added at a final concentration of 1 µM. The R321 peptide was added at final concentrations of 0.05, 0.4, 2.0, and 10.0 µM. Peptide stocks were prepared in DMSO-d_6 and then diluted in PBS, left overnight and centrifuged before addition to the membrane preparation. Samples were loaded into 3 mm NMR tubes (part # S-3-600-7, Norell). ^{1}H-^{13}C HSQC NMR experiments were carried out on a 900-MHz Bruker Avance Spectrometer equipped with a cryogenic probe. Spectral widths in ω1 and ω2 were 8389.262 Hz and 3519.359 Hz, respectively, the transmitter offsets were positioned at 4.7 p.p.m for the ^{1}H dimension and 40 p.p.m. in the ^{13}C dimension. ^{13}C decoupling was performed with a GARP sequence. 256 complex points with 168 scans per FID were recorded, to ensure a 20.9-Hz resolution per point at 900 MHz before zero filling. The relaxation delay was set to 1.5 s and 32 steady-state scans preceded data acquisition. Total collection time was 20 hours. Data were processed and analyzed using the NMRPipe/NMRDraw software [7]. For dissociation constant (K_d) determination, the data were analyzed using Graph Pad Prism 5 non-linear regression saturation single binding site equation. Mean values and standard deviations were calculated based on different fitting approaches (regular fit, robust fit, and automatic outlier).

REFERENCES

1. Provost V, Larose M-C, Langlois A, Rola-Pleszczynski M, Flamand N, Laviolette M. CCL26/eotaxin-3 is more effective to induce the migration of eosinophils of asthmatics than CCL11/eotaxin-1 and CCL24/eotaxin-2. Journal of Leukocyte Biology 2013; 94:213-22.
2. Miyagawa H, Nabe M, Hopp RJ, Okada C, Bewtra AK, G. T. The effect of WEB 2086 on PAF-induced eosinophil chemotaxis and LTC4 production from eosinophils. Agents and actions 1992; 37:39-43.
3. Pinto LH, Eaton E, Chen B, Fleisher J, Shuste D, McCauley R, et al. Gene-environment interactions in a mutant mouse kindred with native airway constrictor hyperresponsiveness. Mammalian Genome 2008; 19:02-14.
4. Holden P, Horton WA. Crude subcellular fractionation of cultured mammalian cell lines. BMC Res Notes 2009; 2:243.
5. Abraham SJ, Kobayashi T, Solaro RJ, Gaponenko V. Differences in lysine pKa values may be used to improve NMR signal dispersion in reductively methylated proteins. J Biomol NMR 2009; 43:239-46.
6. Tripathi A, Vana PG, Chavan TS, Brueggemann LI, Byron KL, Tarasova NI, et al. Heteromerization of chemokine (C-X-C motif) receptor 4 with alpha1A/B-adrenergic receptors controls alpha1-adrenergic receptor function. Proc Natl Acad Sci U S A 2015; 112:E1659-68.
7. Delaglio F, Grzesiek S, Vuister GW, Zhu G, Pfeifer J, Bax A. NMRPipe: a multidimensional spectral processing system based on UNIX pipes. J Biomol NMR 1995; 6:277-93.

FIGURE LEGENDS

Figure S1. R321 does not inhibit platelet-activating factor (PAF)-mediated chemotaxis of human blood eosinophils. Cells treated with 1μM R321, R323, UCB35625, or SB328437 did not exhibit statistically significant reduction of chemotaxis to 1μM PAF. In contrast, the specific PAF receptor inhibitor WEB 2086 achieved 83.18 ± 2.56% inhibition of PAF-mediated chemotaxis in blood eosinophils. Results are shown as percentage of vehicle chemotaxis and represent mean ± SEM from an experiment performed in triplicate. Compared to vehicle: $^{****}p < 0.0001$.

Figure S2. R321 does not induce or promote degranulation with secretion of ECP in human blood eosinophils. CCL11 (12 nM) induces degranulation with secretion of ECP. R321 (1μM) alone does not induce a statistically significant increase in ECP secretion. Cells concurrently treated with CCL11 (12 nM) and 1μM R321, or R323, did not exhibit statistically significant increases in ECP secretion as compared to CCL11-vehicle treated cells. ^{ns}not significant, $^{*}p < 0.05$.

Figure S3. Representative confocal microscopy images of control cells. The first two panels from the top show AML14.3D10-CCR3 cells stained without primary antibodies or with isotype control of primary antibodies. The bottom panel is included as a positive control and represents AML14.3D10-CCR3 cells stained for CCR3 and β-arrestin 2 after 30 min of stimulation with 100nM CCL11.

Figure S4. R321 promotes CCR3 internalization in AML14.3D10-CCR3 cells over a prolonged incubation period. Cells were cultured with vehicle, inhibitors (1µM), and/ or 12 nM CCL11 for a period of 72h. At 24h intervals cells were assessed for surface expression of CCR3 by staining with PE-conjugated anti-CCR3 antibody and measuring median fluorescence via flow cytometry. Results are shown as surface expression of CCR3 as percentage of vehicle expression and represent mean ± SEM from an experiment performed in triplicate. Compared to vehicle: ^{ns} not significant, $*p < 0.05$, $****p < 0.0001$.

Figure S5. Triple allergen (DRA) acute asthma model protocol in Balb/c mice. Allergen sensitization/challenge protocol is indicated. Mice were challenged in their airways with DRA allergen or PBS control on days 12-14 via intranasal insufflation (black arrows). Treatment with CCR3 R321 peptide nanoparticles, scrambled R323 control peptide or vehicle was given: **(A) Prophylactically** starting on day 11 before the i.n. allergen challenges on days 11–14 (**blue arrows**) or **(B) Therapeutically** starting on day 14, after the last i.n. allergen challenge (**red arrows**).

Figure S6. R321 and R323 treatment does not lead to significant changes in total numbers of macrophages, neutrophils, or lymphocytes in lung airways. Total macrophage, neutrophil, and lymphocyte cell numbers in the BAL fluid of triple-allergen (DRA) challenged mice remain unchanged at even the highest doses of R321 and R323. R323 was administered at 12 mg/kg. The mean ± SEM are shown for 6-7 mice/treatment group from 3 independent experiments.

Figure S7. R321 binds CCR3+ membrane preparations in the absence of CCL11. (**A**) Overall strategy to label CCR3 membrane preparations using ^{13}C labeled formaldehyde and borane-ammonia complex. (**B**) ^{13}C HSQC spectra of ^{13}C-reductively methylated CCR3 membrane preparations with signal designations indicated. (**C**) Determination of the dissociation rate constant (K_d) for R321 (0.05-10 µM) binding to CCR3 membrane preparations in the absence of CCL11 shows that R321 affects the intensities of signal 1 and signal 2 with K_d values of 1.604 ± 0.010 µM and 0.014 ± 0.001 µM, respectively, while having no effect on signals 3 and 4 that are present on CCR3 null membranes.

Figure S8. Evaluation of CCL11 binding to CCR3 null membrane preparations. ^{13}C HSQC spectra of ^{13}C-reductively methylated CCR3 null membranes were recorded with 1 µM CCL11. Spectral comparisons between reductively methylated CCR3 null membranes (CCR3-K-di$^{13}CH_3$) (red) and CCR3 null membranes + CCL11 (blue) do not show any signal changes indicative of significant binding. Western blot analysis of membrane preparations from Chem-1 cells overexpressing CCR3 and CCR3 null cells shows the absence of CCR3 expression in the null membranes.

Figure S9. R321 induces concentration-dependent spectral changes in CCR3 membrane preparations. ^{13}C HSQC spectra of ^{13}C-reductively methylated CCR3 membrane preparations were recorded with R321 at 0.05, 0.4, 2.0, 10.0 µM. Spectral comparisons are shown for CCR3 alone (CCR3-K-di$^{13}CH_3$) (**red**) and CCR3 + R321 (**blue**) at (**A**) 0.05 µM, (**B**) 0.4 µM, (**C**) 2.0 µM, (**D**) 10.0 µM, show chemical shift

changes indicative of binding. Black arrows show significant changes in signal line widths and chemical shifts.

Figure S10. Schematic of the CCR3 signaling pathway and proposed R321 mechanism of inhibition. (A) Agonist receptor binding leads to activation of the G-protein dependent signaling cascade resulting in eosinophil chemotaxis, secretion and degranulation. Upon prolonged exposure to agonist, CCR3 is desensitized and internalized via a β-arrestin mediated endocytic pathway. **(B)** R321 nanoparticles dissipate upon contact with the cell membrane, allowing the R321 peptide monomer to displace the CCR3 TM2 helix. R321 binding alters the CCR3 structure in a manner that inhibits G-protein dependent signaling but not β-arrestin-mediated internalization (endocytosis) and degradation of CCR3.

Figure S1

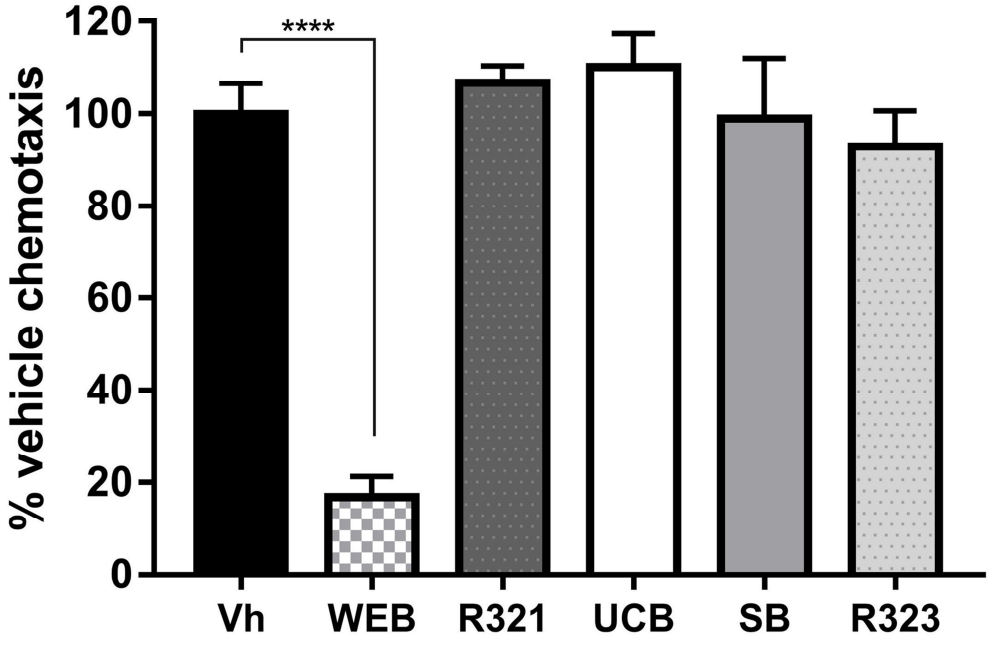
% vehicle chemotaxis
120
100
80
60
40
20
0
****
Vh
WEB
R321
UCB
SB
R323

Figure S2.

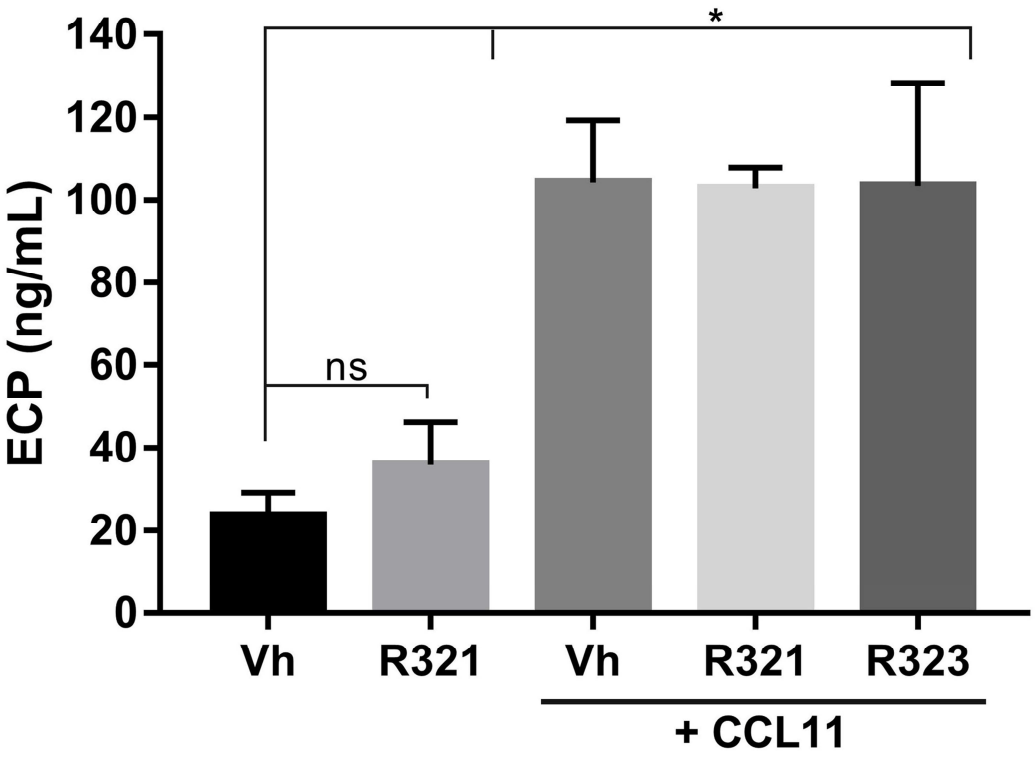

Figure S3

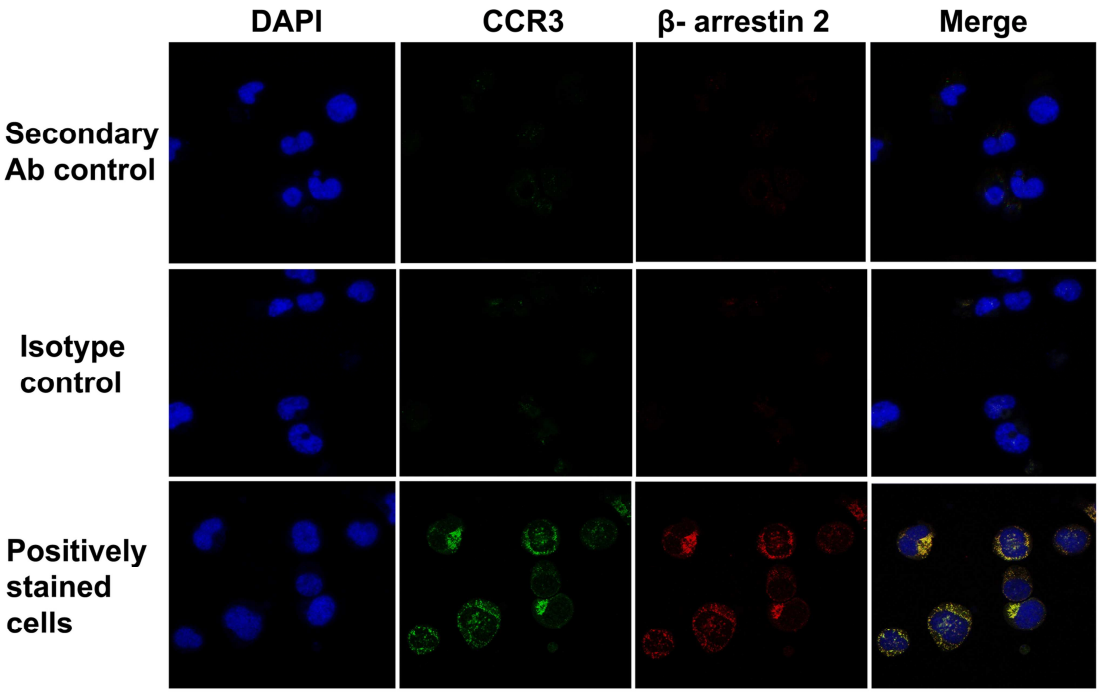
DAPI
CCR3
β- arrestin 2
Merge
Secondary Ab control
Isotype control
Positively stained cells

Figure S4

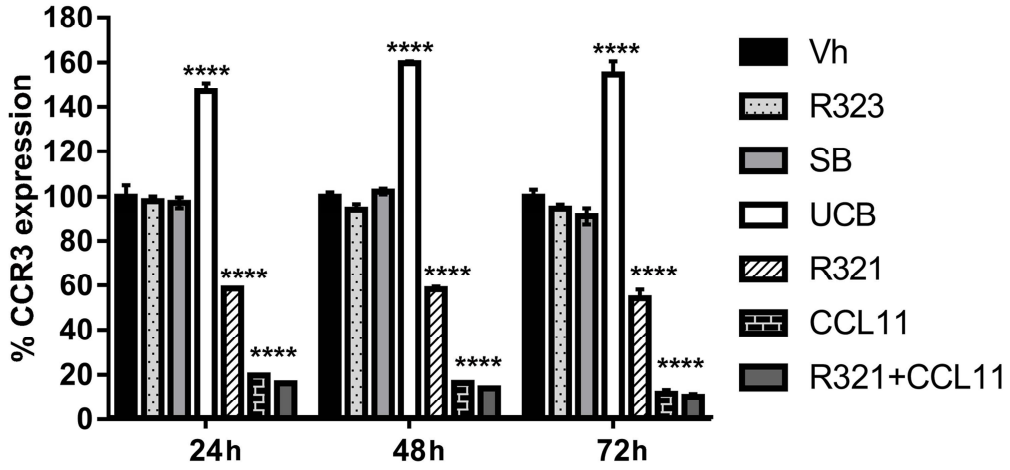
% CCR3 expression
180
160
140
120
100
80
60
40
20
0
****
****
****
****
****
****
24h
48h
72h
Vh
R323
SB
UCB
R321
CCL11
R321+CCL11

Figure S5

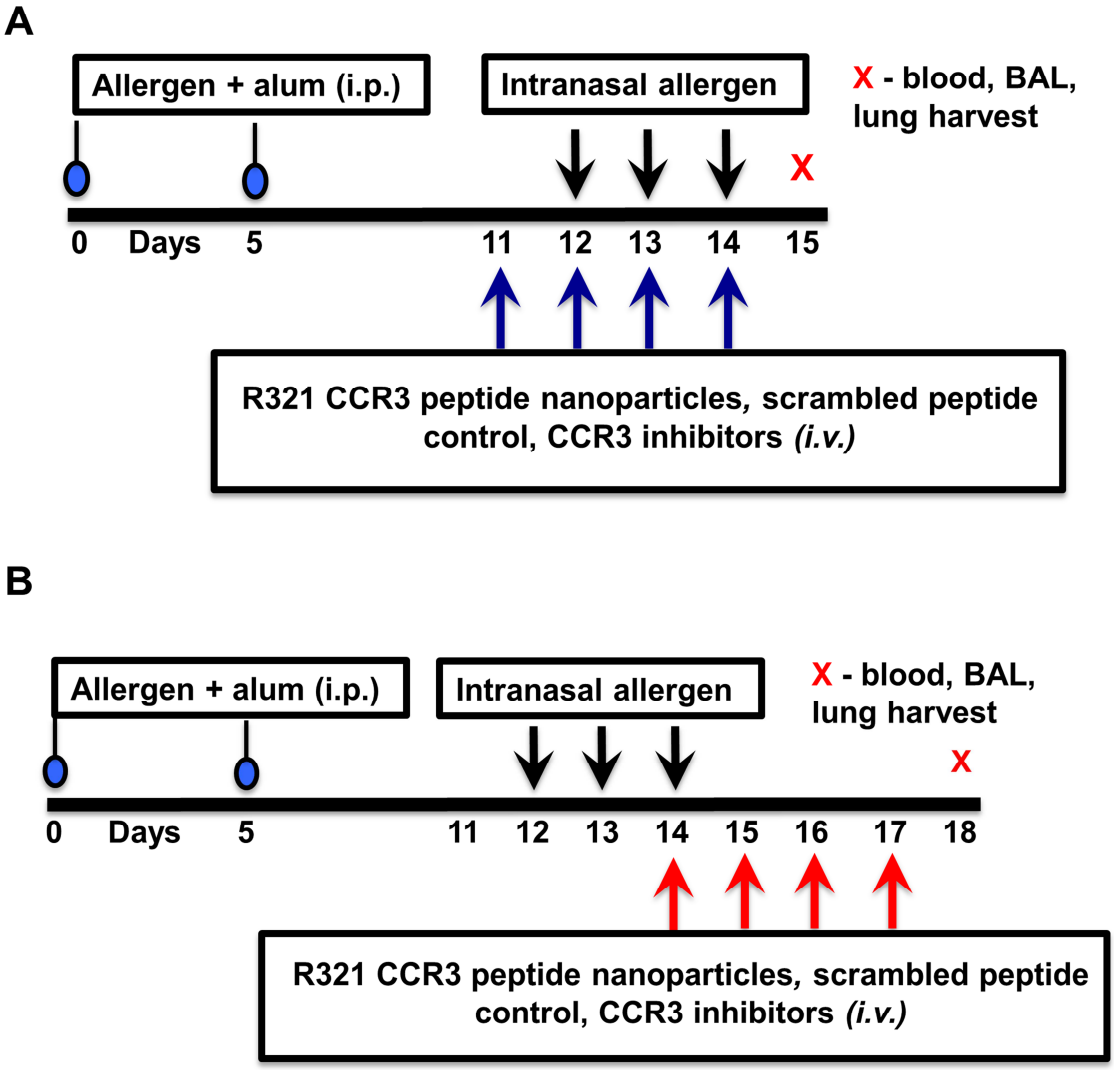
A
Allergen + alum (i.p.)
Intranasal allergen
X - blood, BAL, lung harvest
X
0 Days 5 11 12 13 14 15
R321 CCR3 peptide nanoparticles, scrambled peptide control, CCR3 inhibitors (i.v.)
B
Allergen + alum (i.p.)
Intranasal allergen
X - blood, BAL, lung harvest
X
0 Days 5 11 12 13 14 15 16 17 18
R321 CCR3 peptide nanoparticles, scrambled peptide control, CCR3 inhibitors (i.v.)

Figure S6

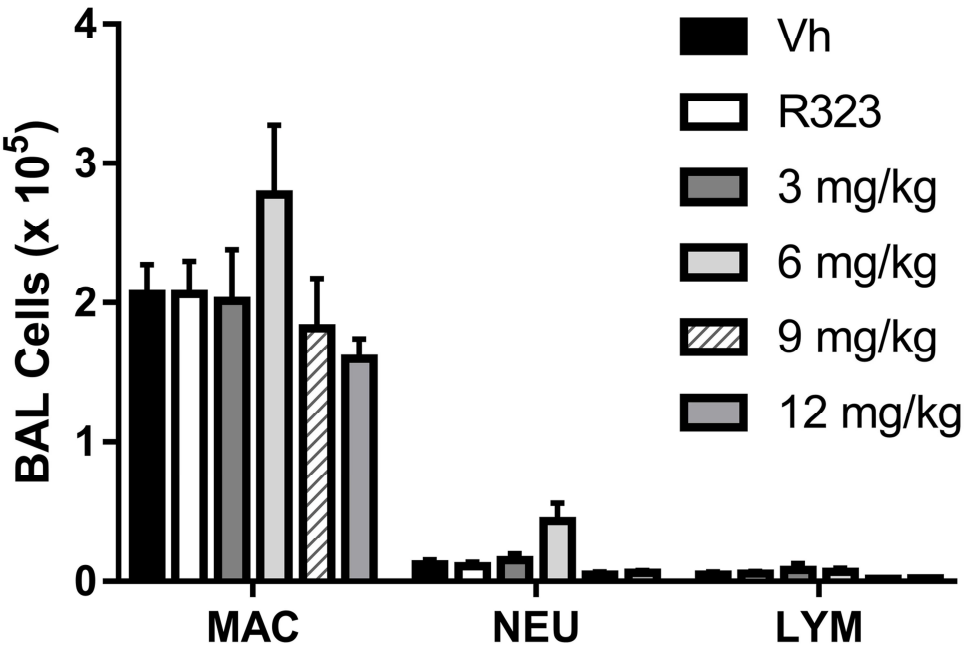
BAL Cells (x 10^5)
4
3
2
1
0
MAC
NEU
LYM
Vh
R323
3 mg/kg
6 mg/kg
9 mg/kg
12 mg/kg

Figure S7

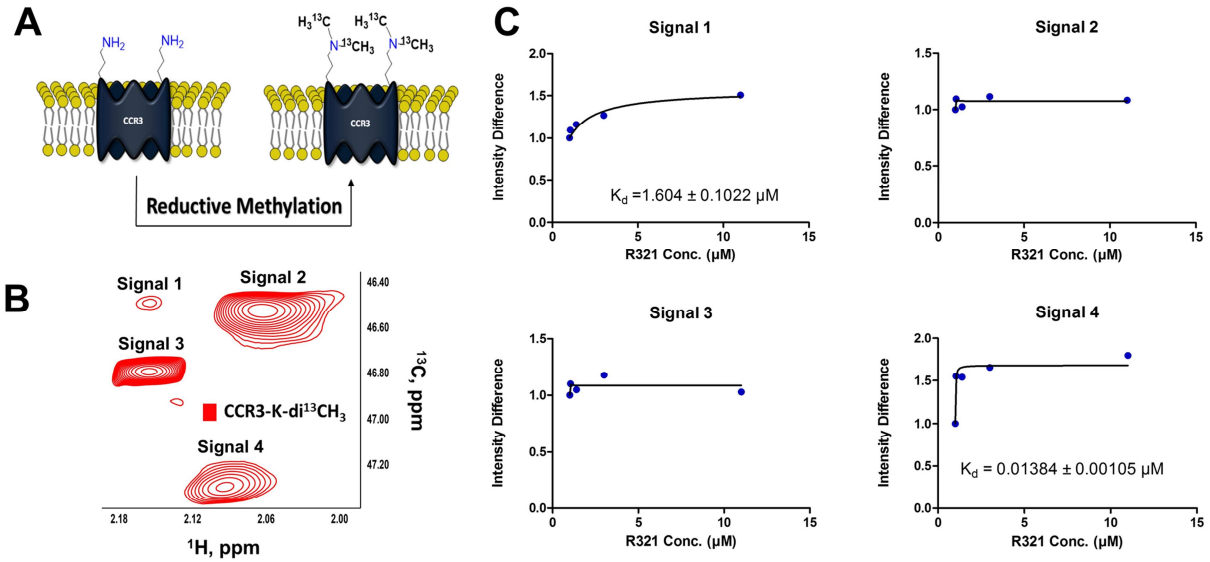
A
NH2
NH2
CCR3
H3 13C
H3 13C
N-13CH3
N-13CH3
CCR3
Reductive Methylation
B
Signal 1
Signal 2
Signal 3
CCR3-K-di13CH3
Signal 4
46.40
46.60
46.80
47.00
47.20
13C, ppm
2.18
2.12
2.06
2.00
1H, ppm
C
Signal 1
Intensity Difference
Kd =1.604 ± 0.1022 μM
R321 Conc. (μM)
Signal 2
Intensity Difference
R321 Conc. (μM)
Signal 3
Intensity Difference
R321 Conc. (μM)
Signal 4
Intensity Difference
Kd = 0.01384 ± 0.00105 μM
R321 Conc. (μM)

Figure S8

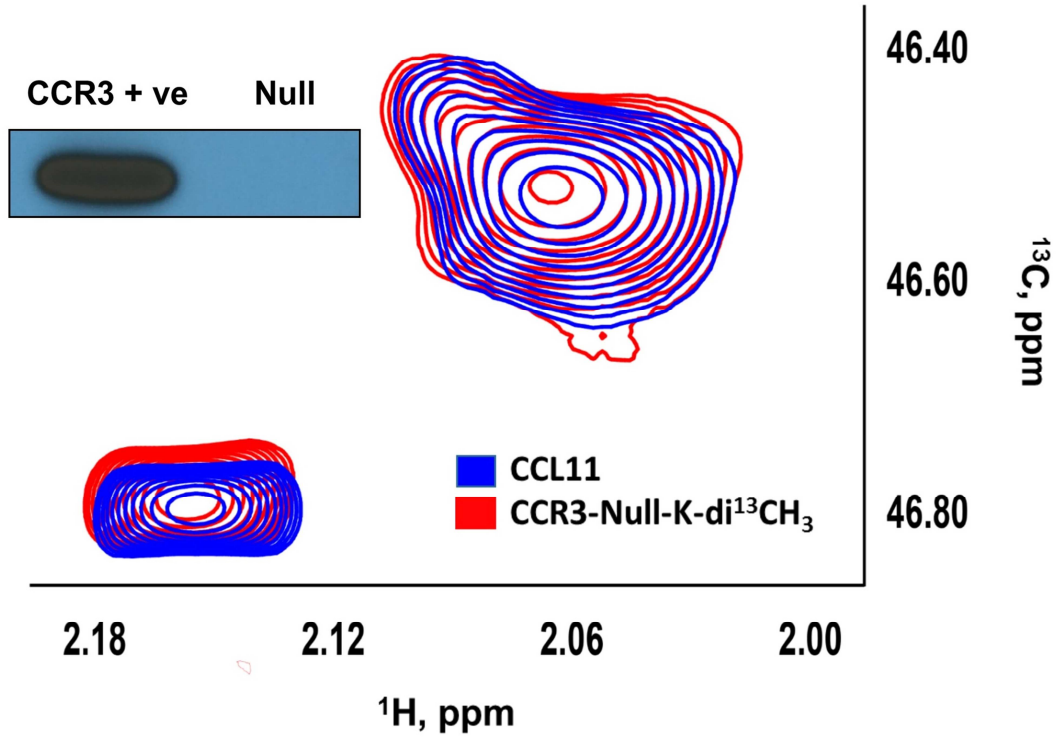
CCR3 + ve
Null
46.40
46.60
46.80
^{13}C, ppm
CCL11
CCR3-Null-K-di^{13}CH$_3$
2.18
2.12
2.06
2.00
^{1}H, ppm

Figure S9

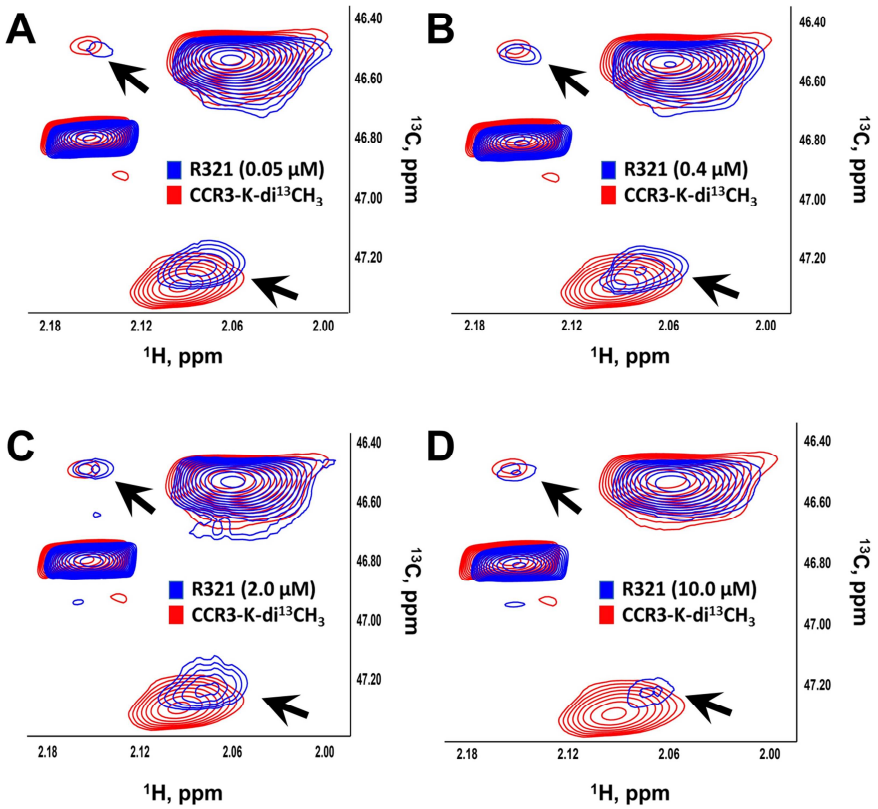
A
B
C
D
R321 (0.05 µM)
R321 (0.4 µM)
R321 (2.0 µM)
R321 (10.0 µM)
CCR3-K-di13CH3
13C, ppm
1H, ppm
46.40
46.60
46.80
47.00
47.20
2.18
2.12
2.06
2.00

Figure S10

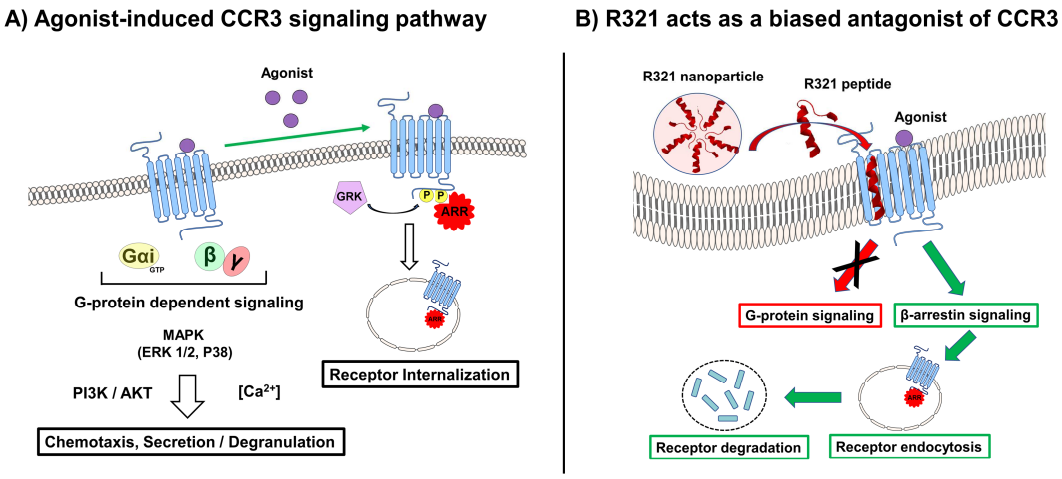
A) Agonist-induced CCR3 signaling pathway
B) R321 acts as a biased antagonist of CCR3
Agonist
GRK
P P
ARR
Gαi
GTP
β
γ
G-protein dependent signaling
MAPK
(ERK 1/2, P38)
PI3K / AKT
[Ca2+]
Chemotaxis, Secretion / Degranulation
Receptor Internalization
R321 nanoparticle
R321 peptide
Agonist
G-protein signaling
β-arrestin signaling
Receptor degradation
Receptor endocytosis